Acta Crystallographica Section D
Biological Crystallography
ISSN 0907-4449

Preliminary X-ray characterization and phasing of a type II cohesin domain from the cellulosome of *Acetivibrio cellulolyticus*

Ilit Noach,[a] Raphael Lamed,[a] Qi Xu,[a] Sonia Rosenheck,[a] Linda J. W. Shimon,[b] Edward A. Bayer[c] and Felix Frolow[a]*

[a]Department of Molecular Microbiology and Biotechnology, George S. Wise Faculty of Life Sciences, Tel Aviv University, Ramat Aviv 68790, Israel, [b]Department of Chemical Services, The Weizmann Institute of Science, Rehovot 76100, Israel, and [c]Department of Biological Chemistry, The Weizmann Institute of Science, Rehovot 76100, Israel

Correspondence e-mail: felixf@tauex.tau.ac.il

Received 12 May 2003
Accepted 18 June 2003

The N-terminal type II cohesin from the cellulosomal ScaB subunit of *Acetivibrio cellulolyticus* was crystallized in two different crystal systems: orthorhombic (space group $P2_12_12_1$), with unit-cell parameters $a = 37.455$, $b = 55.780$, $c = 87.912$ Å, and trigonal (space group $P3_121$), with unit-cell parameters $a = 55.088$, $b = 55.088$, $c = 112.553$ Å. The two crystals diffracted to 1.2 and 1.9 Å, respectively. A selenomethionine derivative was also crystallized and exhibited trigonal symmetry (space group $P3_121$), with unit-cell parameters $a = 55.281$, $b = 55.281$, $c = 112.449$ Å and a diffraction limit of 1.97 Å. Initial phasing of the trigonal crystals was successfully performed by the SIRAS method using Cu $K\alpha$ radiation with the selenomethionine derivative as a heavy-atom derivative. The structure of the orthorhombic crystal form was solved by molecular replacement using the coordinates of the trigonal form.

1. Introduction

Cellulosomes are multi-enzyme complexes produced by anaerobic cellulolytic bacteria that efficiently degrade cellulose and other plant cell-wall polysaccharides (Bayer *et al.*, 1998; Beguin & Lemaire, 1996; Felix & Ljungdahl, 1993; Lamed & Bayer, 1988; Schwarz, 2001; Shoham *et al.*, 1999). The cellulosome complex contains a primary scaffoldin subunit that incorporates the enzyme subunits into the complex and, in some bacterial systems, one or more anchoring proteins that mediate attachment of the cellulosome to the cell surface.

The assembly of cellulosomal subunits into the mature complex is dictated by a tenacious interaction between two complementary types of module: the cohesin and the dockerin. The cohesins are currently classified into several types, distinguished by relatively minor sequence differences. Thus far, the crystal structures of three different type I cohesins have been elucidated from the primary cellulosomal scaffoldins of *Clostridium thermocellum* and *C. cellulolyticum* (Shimon, Bayer *et al.*, 1997; Shimon, Frolow *et al.*, 1997; Spinelli *et al.*, 2000; Tavares *et al.*, 1997). In addition, the preliminary chemical shifts and secondary-structure assignment of a type II cohesin from the *C. thermocellum* anchoring protein SdbA have recently been reported (Smith *et al.*, 2002). A solution structure of a *C. thermocellum* dockerin domain has also been published (Lytle *et al.*, 2001).

The cellulosomal system of *Acetivibrio cellulolyticus* contains a primary scaffoldin, ScaA (CipV), and at least two anchoring proteins, ScaB and ScaC (Ding *et al.*, 1999; Xu *et al.*, 2003). The cohesins from these three proteins are all different; *i.e.* the ScaA cohesins are of type I, those from ScaB are of type II and the ScaC cohesins are of yet another type. In the present communication, we describe the crystallization and preliminary X-ray characterization of a type II cohesin from *A. cellulolyticus* ScaB.

2. Materials and methods

2.1. Overexpression of native cohesin

The DNA encoding the N-terminal cohesin (cohesin B1) from the *scaB* scaffoldin gene of *A. cellulolyticus* was cloned into the pET28a expression vector (Novagen) together with a sequence encoding for a His tag attached to the 3′ end using restriction enzymes *Nco*I and *Xho*I; the resultant plasmid was transferred to *Escherichia coli* strain BL21. A single colony was transferred into 100 ml of LB medium containing 25 µg ml^{-1} of kanamycin and grown overnight with shaking (250 rev min^{-1}). When the growth culture (2 l) reached an A_{600} of 0.6, 0.1 m*M* isopropyl-β-D-thiogalactopyranoside (IPTG) was added to induce gene expression and cultivation was continued at 310 K for an additional 12 h. Cells were then harvested by centrifugation (6000 rev min^{-1} for 10 min) at 277 K. Cells were resuspended in 50 m*M* NaH_2PO_4 pH 8.0 containing 300 m*M* NaCl at a ratio of 1 g wet pellet to 4 ml buffer solution. Prior to sonication, 1 m*M* of phenylmethylsulfonyl fluoride (PMSF) was added along with a few micrograms of DNase powder. The suspension was kept on ice during sonication, after which the suspension was centrifuged (15 000 rev min^{-1} at 277 K for 20 min) and the

supernatant fluids were collected. The expressed His-tagged protein was isolated by metal-chelate affinity chromatography using a nickel–nitrilotriacetic acid (Ni–NTA) resin. Fast protein liquid chromatography (FPLC) was performed using a Superdex HR 10/30 column and FPLC system (Pharmacia, Uppsala, Sweden). The purified fractions were collected and diluted by a factor of 5 with double-distilled water. The protein was concentrated using Centiprep Centrifugal Filter Devices YM-3 (Amicon Bio-separation, Millipore), yielding 3 ml of purified concentrated cohesin B1. Protein concentration was determined by measuring the absorbance spectrum (ε_{280} = 12 090).

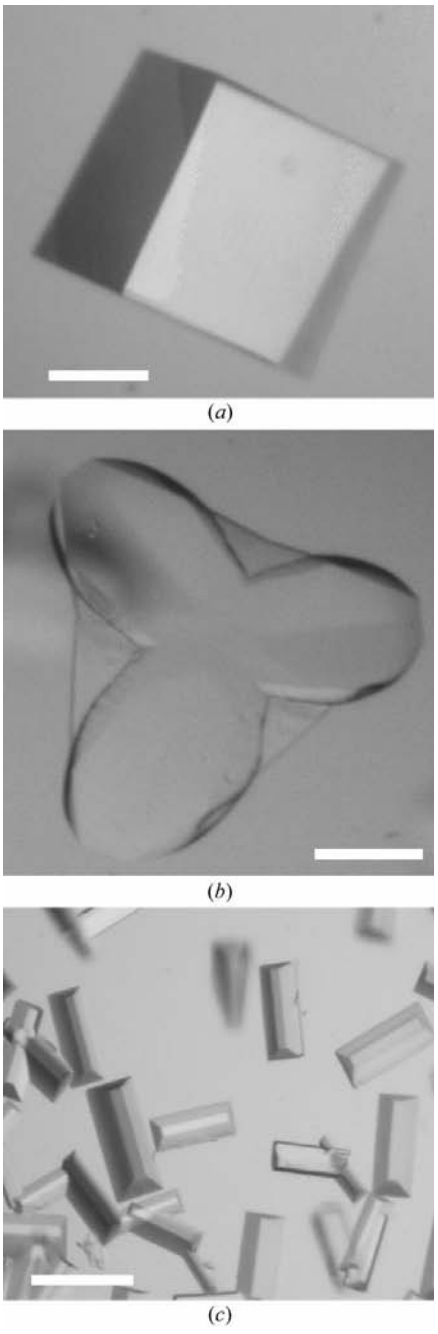

Figure 1
Crystals of cohesin B1 (the N-terminal type II cohesin from the cellulosomal ScaB subunit) from *A. cellulolyticus*. (*a*) The native cohesin, trigonal form; (*b*) the SeMet derivative, trigonal form; (*c*) the native cohesin, orthorhombic form. The white bar corresponds to approximately 0.1 mm.

Native cohesin B1 crystals were crystallized at 293 K by the hanging-drop vapour-diffusion method. Initial crystallization experiments were based on the sparse-matrix sampling method using Hampton Research Crystal Screen I. The protein solution (2 µl of a 10.8 mg ml^{-1} solution in 10 m*M* Tris pH 7.5, 0.03 *M* NaCl and 0.01% sodium azide) was mixed with an equal volume of reservoir solution and equilibrated against 0.4 ml of precipitant solution in a 24-well Linbro plate. Crystals were obtained under two conditions: Nos. 32 (2.0 *M* ammonium sulfate) and 47 (2.0 *M* ammonium sulfate and 0.1 *M* sodium acetate trihydrate pH 4.6). Crystals derived from condition No. 32 appeared as equidimensional trigonal prisms and grew to a final size of 0.4 mm in 7 d (Fig. 1*a*); crystals from condition No. 47 grew to final dimensions of 0.14 × 0.06 × 0.06 mm in 2 d (Fig. 1*c*) and exhibited an orthorhombic morphology.

2.2. Overexpression of SeMet derivative

The above-mentioned plasmid used for overproduction of native cohesin B1 was used to transform *E. coli* B834(DE3)pLysS cells (Novagen). A single colony was precultured for 7 h in 4 ml of LB medium containing 25 µg ml^{-1} kanamycin. The culture was diluted by a factor of 2000 in two steps in M10 minimal medium supplemented with glucose (8 mg ml^{-1}), 80 µg ml^{-1} each of all the common amino acids except methionine, 80 µg ml^{-1} seleno-L-methionine (SeMet) and 25 µg ml^{-1} kanamycin. Protein expression was induced with 0.1 m*M* IPTG and the final culture (2 l) was grown at 310 K. The SeMet protein was purified and concentrated as described for the native protein. During purification of the SeMet protein, all buffers were degassed before application to the Ni–NTA column. The purified fraction was supplemented with 1 m*M* dithiothreitol (DTT) and 0.2 m*M* EDTA to avoid oxidation of SeMet to its selenoxide equivalent. SeMet crystals of cohesin B1 were obtained by the hanging-drop vapour-diffusion method, using the highly purified and concentrated SeMet preparation (10.8 mg ml^{-1} in 10 m*M* Tris–HCl pH 7.5 containing 0.03 *M* NaCl and 0.01% sodium azide). Crystallization was performed using a Hampton Research ammonium sulfate grid screen to explore various ammonium sulfate concentrations and the various buffers employed in this kit. After an initial trial and one round of optimization, final crystallization conditions were established, consisting of 2.0 *M* ammonium sulfate, 0.1 *M* MES pH 6.0, that consistently produced large (∼0.4 × 0.3 × 0.15 mm) crystals of clover-leaf shape (Fig. 1*b*).

2.3. Mass-spectrometry analysis

Samples of the purified native cohesin and its SeMet derivative were subjected to electrospray mass-spectrometric analysis. The molecular-mass difference between the SeMet and the native cohesin B1 was determined to be 161.26 mass units. This value corresponds to an average content of 3.4 Se atoms per molecule of the labelled protein and is consistent with the four Met residues present in cohesin 1 (or three Met residues, taking into account partial removal of the N-terminal residue).

2.4. Data collection and processing

To check crystal diffraction quality, trigonal crystals of the native and the SeMet protein were loaded into sealed thin-wall glass capillaries and mounted on an ULTRAX18 rotating-anode generator equipped with a 0.3 mm focal cup, OSMIC multi-layer confocal mirrors and an R-AXIS IV area detector. Data were collected using Cu $K\alpha$ radiation (1.5418 Å) at a temperature of 293 K to resolutions of 1.90 and 1.97 Å for the native protein and the SeMet derivative, respectively. The crystals belong to the trigonal space group $P3_121$ (or $P3_221$), with unit-cell parameters $a = b = 55.09$, $c = 112.55$ Å, $\alpha = \beta = 90.0$, $\gamma = 120^\circ$ and $a = b = 55.28$, $c = 112.45$ Å, $\alpha = \beta = 90.0$, $\gamma = 120^\circ$ for the native and SeMet crystals, respectively.

Orthorhombic crystals of cohesin B1 were measured using synchrotron radiation (ID14-EH1 beamline station at ESRF, Grenoble, France). An ADSC detector and X-ray radiation of 0.934 Å wavelength were used. The crystal, incubated for a fraction of a minute in a solution mimicking the mother liquor with addition of 25% ethylene glycol, was mounted in a cryoloop (Teng, 1990) and placed in a stream of cold nitrogen at a temperature of 100 K generated by an Oxford Cryosystems cryostream (Cosier & Glazer, 1986). The crystals had orthorhombic symmetry, with unit-cell parameters a = 37.455, b = 55.780, c = 87.912 Å,

Table 1
Data-collection and processing statistics for cohesin B1 crystals.

Values in parentheses are for the highest resolution shell.

	Trigonal form		Orthorhombic form
	Native1	SeMet	Native2
Experimental conditions			
X-ray source	ULTRAX18 rotating anode	ESRF (ID14-EH1 station)	
Wavelength (Å)	1.5418 (Cu $K\alpha$)	1.5418 (Cu $K\alpha$)	0.934
Temperature (K)	293	293	100
Detector	R-AXIS IV	R-AXIS IV	ADSC
Crystal parameters			
Space group	$P3_121$	$P3_121$	$P2_12_12_1$
Unit-cell parameters			
a (Å)	55.088	55.281	37.455
b (Å)	55.088	55.281	55.780
c (Å)	112.553	112.449	87.912
α (°)	90	90	90
β (°)	90	90	90
γ (°)	120	120	90
Resolution (Å)	1.90 (1.93–1.90)	1.97 (2.00–1.97)	1.20 (1.22–1.20)
Mosaicity (°)	0.342	0.322	0.293
V_M (Å^3 Da^{-1})	2.5	2.5	2.6
Solvent content (%)	59.9	59.9	58.2
Asymmetric unit (monomers)	1	1	1
Data processing			
No. observed reflections	123084	133211	225393
No. unique reflections	16221	14752	58341
Completeness (%)	99.8 (99.1)	99.8 (99.7)	95.8 (99.1)
R_{sym}†	0.072 (0.662)	0.081 (0.587)	0.046 (0.172)
$I/\sigma(I)$	23.9 (2.0)	23.3 (2.3)	13.3 (4.0)

† $R_{sym} = \sum |I - \langle I \rangle| / \sum I$.

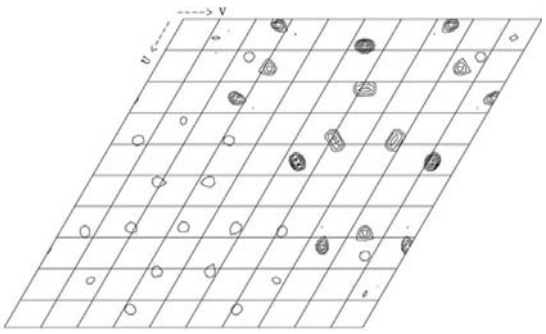

Figure 2
Isomorphous Patterson map (w = 0.33333 section) calculated at 46–2.0 Å resolution.

$\alpha = \beta = \gamma = 90°$. Data were collected to 1.2 Å resolution.

Data for both crystalline forms were collected in 1° oscillation frames and were processed with *DENZO* and *SCALEPACK* (Otwinowski & Minor, 1997) (Table 1).

The presence of only one monomer in the asymmetric unit for both trigonal and orthorhombic forms (corresponding to solvent contents of 59.9 and 58.2%, respectively) was supported by calculated Matthews coefficients of 2.6 and 2.5 Å^3 Da^{-1}, respectively (Matthews, 1968), and self-rotation functions, calculated by *POLARRFN* (Collaborative Computational Project, Number 4, 1994), that showed no significant peaks.

2.5. Phasing

Initial inspection of diffraction data collected from trigonal crystals of the native and SeMet preparations revealed a high degree of isomorphism between the native and SeMet crystals (data not shown). Three Se atoms were clearly visible in the isomorphous (Fig. 2) and anomalous (data not shown) Patterson synthesis maps. Their positions were determined using data between 46 and 2.0 Å resolution by manual interpretation of the Patterson function with the aid of *RSPS* (Collaborative Computational Project, Number 4, 1994; Knight, 2000) and confirmed by automatic procedures implemented in *SOLVE* (Terwilliger & Berendzen, 1999). Ambiguity in the space-group selection ($P3_121$ *versus* $P3_221$) was resolved by *SOLVE*. Heavy-atom refinement and phasing to 1.97 Å resolution was performed using *MLPHARE* (Collaborative Computational Project, Number 4, 1994). This resulted in phases with a figure of merit of 0.21. Phases were modified and extended to 1.90 Å resolution using standard options of the *DM* program (Collaborative Computational Project, Number 4, 1994; Cowtan & Main, 1998), yielding a figure of merit of 0.82 and an interpretable electron-density map. This map was traced using methods implemented in the program *O* (Jones *et al.*, 1991). Several loop regions in the molecule resisted interpretation and a partial model was used to solve the orthorhombic structure using the program *MOLREP* (Collaborative Computational Project, Number 4, 1994; Vagin & Teplyakov, 1997). Difficult regions were easily traced in the orthorhombic structure and the coordinates were transformed back to the trigonal system.

3. Discussion

Molecular-replacement methods failed to solve both the trigonal and the orthorhombic structures of *A. cellulolyticus* cohesin B1 using the known type I cohesin structures (practically all known molecular-replacement programs and packages were used without success). As an alternative solution, the MAD method was considered and an SeMet derivative was therefore overexpressed, purified, concentrated and crystallized.

In spite of the similarity in crystallization conditions, space group and unit-cell parameters between the SeMet derivative and the native protein (Table 1), the SeMet crystals exhibited a very different morphology (Fig. 1). Prior to shipping of the SeMet crystals to the synchrotron, their quality was checked using in-house equipment. The native and SeMet crystals appeared to be highly isomorphous and both diffracted to similar levels of resolution, thus indicating that the presence of SeMet did not corrupt the crystal quality. In order to examine the success of SeMet derivatization, isomorphous and anomalous Patterson synthesis maps were calculated and the presence of three Se sites was demonstrated unequivocally.

Structures were solved by a combination of SIRAS and molecular-replacement methods. A ribbon diagram rendered from the current coordinates of the type II cohesin molecule from the *A. cellulolyticus* cellulosomal ScaB subunit is shown in Fig. 3. Two short helical elements are clearly visible in the latter structure: one internally located and one at the C-terminus of the molecule. Both of these helices were lacking in the known type I cohesin structures derived from the primary scaffoldins of *C. thermocellum* and *C. cellulolyticum*. In this context, it is interesting to note that only the internal helix between β-strands 6 and 7 was observed in recent solution-structure studies of another type II cohesin derived from the *C. thermocellum* SdbA anchoring protein (Smith *et al.*, 2002). In the present work, 13

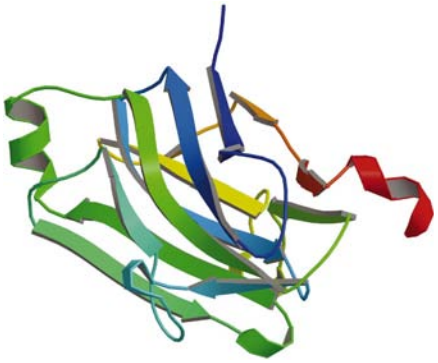

Figure 3
Ribbon diagram of the type II cohesin B1 molecule from *A. cellulolyticus* ScaB. The figure was created using *MOLSCRIPT* (Kraulis, 1991) and rendered using *Raster3D* (Merritt & Murphy, 1994).

additional residues not reported for the solution structure of the *C. thermocellum* SdbA cohesin form an extended strand and an additional helix (Fig. 3). Refinement of the trigonal and orthorhombic structures of the type II cohesin from *A. cellulolyticus* ScaB is now in progress.

We gratefully acknowledge the ESRF for synchrotron beam time and the staff scientists of the ID14-1 station for their assistance. IN acknowledges Tel Aviv University for an MSc student scholarship. This work was supported by the Israel Science Foundation (No. 133-00 to RL and 771-01 to EAB), the US–Israel Binational Agricultural Research and Development Fund (BARD Research Grant No. 3106-99C) and by a grant from the United States–Israel Binational Science Foundation (BSF).

References

Bayer, E. A., Chanzy, H., Lamed, R. & Shoham, Y. (1998). *Curr. Opin. Struct. Biol.* **8**, 548–557.
Beguin, P. & Lemaire, M. (1996). *Crit. Rev. Biochem. Mol. Biol.* **31**, 201–236.
Collaborative Computational Project, Number 4 (1994). *Acta Cryst.* D**50**, 760–763.
Cosier, J. & Glazer, A. M. (1986). *J. Appl. Cryst.* **19**, 105–107.
Cowtan, K. & Main, P. (1998). *Acta Cryst.* D**54**, 487–493.
Ding, S.-Y., Bayer, E. A., Steiner, D., Shoham, Y. & Lamed, R. (1999). *J. Bacteriol.* **181**, 6720–6729.
Felix, C. R. & Ljungdahl, L. G. (1993). *Annu. Rev. Microbiol.* **47**, 791–819.
Jones, T. A., Zou, J. Y., Cowan, S. W. & Kjeldgaard, M. (1991). *Acta Cryst.* A**47**, 110–119.
Knight, S. D. (2000). *Acta Cryst.* D**56**, 42–47.
Kraulis, P. J. (1991). *J. Appl. Cryst.* **24**, 946–950.
Lamed, R. & Bayer, E. A. (1988). *Adv. Appl. Microbiol.* **33**, 1–46.
Lytle, B. L., Volkman, B. F., Westler, W. M., Heckman, M. P. & Wu, J. H. D. (2001). *J. Mol. Biol.* **307**, 745–753.
Matthews, B. W. (1968). *J. Mol. Biol.* **33**, 491–497.
Merritt, E. A. & Murphy, M. E. P. (1994). *Acta Cryst.* D**50**, 869–873.
Otwinowski, Z. & Minor, W. (1997). *Methods Enzymol.* **276**, 307–326.
Schwarz, W. H. (2001). *Appl. Microbiol. Biotechnol.* **56**, 634–649.
Shimon, L. J. W., Bayer, E. A., Morag, E., Lamed, R., Yaron, S., Shoham, Y. & Frolow, F. (1997). *Structure*, **5**, 381–390.
Shimon, L. J. W., Frolow, F., Yaron, S., Bayer, E. A., Lamed, R., Morag, E. & Shoham, Y. (1997). *Acta Cryst.* D**53**, 114–115.
Shoham, Y., Lamed, R. & Bayer, E. A. (1999). *Trends Microbiol.* **7**, 275–281.
Smith, S. P., Beguin, P., Alzari, P. M. & Gehring, K. (2002). *J. Biomol. NMR*, **23**, 73–74.
Spinelli, S., Fierobe, H. P., Belaich, A., Belaich, J. P., Henrissat, B. & Cambillau, C. (2000). *J. Mol. Biol.* **304**, 189–200.
Tavares, G. A., Beguin, P. & Alzari, P. M. (1997). *J. Mol. Biol.* **273**, 701–713.
Teng, T.-Y. (1990). *J. Appl. Cryst.* **23**, 387–391.
Terwilliger, T. C. & Berendzen, J. (1999). *Acta Cryst.* D**55**, 849–861.
Vagin, A. & Teplyakov, A. (1997). *J. Appl. Cryst.* **30**, 1022–1025.
Xu, Q., Gao, Ding, S.-Y., Kenig, R., Shoham, Y., Bayer, E. A. & Lamed, R. (2003). In the press.